



# Influence of the application of ultrasound on the microstructure of cemented carbide/steel joints brazed with Ag49ZnCuMnNi

L. Wojarski<sup>1</sup> · W. Tillmann<sup>2</sup> · H. Ulitzka<sup>2</sup> · T. Ulitzka<sup>1</sup>

Received: 28 October 2022 / Accepted: 26 July 2023  
© The Author(s) 2023

## Abstract

The poor wettability of cemented carbides by molten metals as well as the different material properties compared to steel makes thermal joining process challenging. In this regard, innovative ultrasonic-assisted induction brazing is capable of joining the materials quickly, cost-effectively and without using environmentally hazardous fluxes. Instead, the oxide scales are broken up within the joining process due to ultrasonic-induced cavitation in the molten filler alloy and hence promote the wetting. However, since the use of ultrasound in brazing steel/cemented carbide joints is still insufficiently investigated, there is still a need to explore the fundamental influences of ultrasound on the brazing process. In this work, the effect of ultrasound on the microstructure of the brazed joints and the diffusion depth of different elements were analysed. The two ultrasonic parameters activation time and amplitude were varied during the experiments. Acicular or dendritic structures that have formed in the braze metal without ultrasonic stimulation were transformed into globular structures, when ultrasound was applied. In addition, a non-eutectic silver-rich phase formed, which was not observed in joints manufactured without the use of ultrasound. Furthermore, the use of ultrasound led to increased diffusion between the base material and the filler material as well as the dissolution and distribution of oxides in the edge regions of the brazing joints.

**Keywords** Ultrasonic-assisted brazing · Cemented carbide · Steel · Microstructure · Joint strength · Wetting · Connectivity

## 1 Introduction

Cemented carbide is a widely used cutting material due to its favourable ratio of hardness to ductility. Cemented carbide is used in metal cutting, rock machining and forming processes. Due to the high price of cemented carbide and low ductility, tools are rarely made entirely of cemented carbide. In most cases, steel alloys serve as the base material on which a cutting edge made of cemented carbide is applied. A screw or clamp connection is usually used to fasten the cemented carbide for simple tool geometries. For more complicated or small geometries, thermal joining is favourable. Due to the significant differences in the coefficients of

thermal expansion, welding of steel and cemented carbide is only suitable for processes in which the heat can be introduced precisely. These processes include resistance welding as well as laser beam welding [1, 2]. In contrast to welding, the heat input into the joining partners during brazing is significantly lower. Brazing of steel/cemented carbide joints can be carried out in an inert or oxygen-rich atmosphere or vacuum, which involves higher investment and process costs compared to brazing in air [3–5]. But brazing in an oxygen-rich atmosphere leads to the formation of oxide scales on the surface of the joining partners and hence the necessity of the usage of fluxes. But fluxes are environmentally harmful, toxic and can lead to defects in the brazing seam [6]. As an alternative to fluxes, power ultrasound supports the brazing of light metals such as titanium or aluminium. This generates cavitation in the molten filler material during the brazing process. The cavitation destroys the oxide layers during the brazing operation and enhances their pouring into the edge areas of the joining couple [7].

The positive influence of power ultrasound during brazing of steel-cemented carbide joints on strength and wetting was demonstrated in [8] and [9]. In [8], the strength increase

---

Recommended for publication by Commission XVII - Brazing, Soldering and Diffusion Bonding

---

✉ L. Wojarski  
lukas.wojarski@tu-dortmund.de

<sup>1</sup> Lehrstuhl Für Werkstofftechnologie, TU Dortmund, Dortmund, Germany

<sup>2</sup> RIF E.V, Dortmund, Germany

**Table 1** Chemical composition of the 1.2210 (wt%)

1.2210	C	Si	Mn	Cr	V	Fe
	1.2	0.2	0.3	0.7	0.1	Rest

**Table 2** Chemical composition of the K40 (wt%)

K40	W	Co
	88	12

**Table 3** Chemical composition of the Ag449 (wt%)

Ag449	Ag	Cu	Zn	Mn	Ni
	49.0	16.0	23.0	7.5	4.5

was attributed to the ultrasound-stimulated migration of WC particles into the brazed joint. It was suggested by Li that the WC particles hindered the crack propagation in the brazing seam. In [9], no pronounced migration of WC particles into the brazing seam was detected. However, it was observed that as the activation time of ultrasound increased, the wetting of the base materials improved, too, and the ratio of oxides within the brazing seam decreased. In [10], Jiang et al. studied the microstructure of steel-cemented carbide joints brazed with a silver-based filler metal and found a correlation between the distribution of phases and the strength of the joint. Since the use of power ultrasound during brazing affects the phase distribution and grain size of the microstructure in the brazed joint [11, 12], a study of the microstructure is essential to provide a fundamental understanding of the joining process influence on the resulting joint properties. Within this work, the effect of power ultrasound during the brazing process on the distribution of phases and elements in the brazing seam has been investigated. Power ultrasound is defined as ultrasound that has an effect on the structure of the component it is applied to. The experiments were performed with different activation times and amplitudes of ultrasound. The microstructure of the brazing seam in the cross section as well as in the fracture surface was investigated.

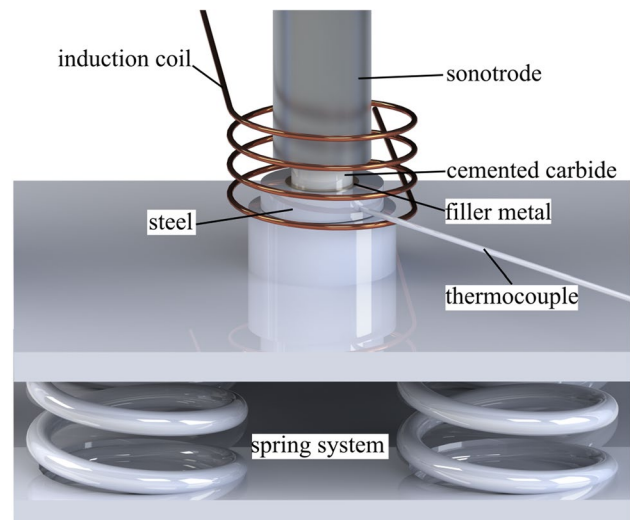
## 2 Experimental procedure

### 2.1 Brazing materials

The filler alloy Ag449 has been used to join the steel 1.2210 and the carbide grade K40. The 1.2210 is a cold work steel that is frequently used in cutting and forming processes. Its chemical composition is summarized in Table 1. The K40 carbide grade is used for machining non-ferrous metals, cast materials and wood. The Co-binder content is 88%, and the grain size of WC amounts 1.5  $\mu\text{m}$  (Table 2). The composition of the silver filler metal Ag449 is shown in Table 3. The filler metal has a melting range between 680 and 705  $^{\circ}\text{C}$ . For the brazing experiments, the following geometries were selected for the materials (Table 4).

**Table 4** Geometries of the materials

Material	Diameter (mm)	Thickness (mm)
1.2210	20	4
K40	10	4
Ag449	12	0.2

**Fig. 1** Setup of the brazing stand

### 2.2 Brazing procedure

The substrates were assembled in the butt joint configuration in the test device, and an external force of 200 N was applied via a spring system (see Fig. 1). An effect of the spring system on the resonance did not occur. The position of the steel was fixed in a steel cylinder with a groove. Heating was provided by an induction furnace in air, and the temperature was controlled by a thermocouple that was attached to the steel substrate. The assembly was heated to the joining temperature of 790  $^{\circ}\text{C}$  with a heating rate of 10 K/s, and the temperature was held for 15 s. When

the brazing temperature was reached, the ultrasound was activated and held for 5 resp. 25 s. The amplitude of the ultrasound was varied between 19 and 38  $\mu\text{m}$ . After the isothermal hold, the joint cooled down in air. For benchmarking reasons, reference samples were brazed without the use of ultrasound so that a total of five parameter variations were investigated within this paper.

### 2.3 Analytical methods

For the microstructural examination of the joints, a transverse cross section has been prepared. The preparation of the samples included grinding, polishing and etching of the samples. Furthermore, one-lap shear tests were performed with the setup described in [13]. For each parameter, three samples were tested and cross sections of the fractured samples parallel to the fracture mirror were prepared. The cross sections were investigated with a scanning electron microscope (JSM 7001F) equipped with an EDS. Furthermore, the bond quality was determined by ultrasonic immersion testing (Vogt, LS100). The used probe had a frequency of 25 MHz. For the adjustment of the non-destructive test technique, an unbrazed couple consisting of the steel and the cemented carbide substrate was used. The reflection of the control sample was adjusted to a value of 80%.

## 3 Results and discussion

### 3.1 Microstructure

The microstructure of the sample brazed without the application of ultrasound consists of large area phases (1) that are embedded in a fine eutectic phase mixture (2) (see Fig. 2). The dark grey large area phases are poor in Ag and mainly

consist of Mn, Ni, Cu and Zn. They feature a dendritic structure. The eutectic phase mixture is rich in Ag, Zn and Cu and contains only small amounts of Ni, Mn and O (Table 5). Its constituents feature an acicular shape.

The application of ultrasound affects the microstructure of the brazing seam depending on the chosen parameters for the activation time and the amplitude of the ultrasound as clearly visible in Fig. 3. In comparison to the sample brazed without the application of ultrasound, the appearance of the microstructures of the samples brazed with ultrasonic stimulation differs significantly. The microstructure of the sample with a low amplitude (19  $\mu\text{m}$ ) and activation time (5 s) of the ultrasound still consists of the dark grey large area phase (1) and fine eutectic phase mixture (2) (see Fig. 3A). But the silver-poor dark grey phase does not feature a dendritic structure anymore. It has a globular shape. In contrast, the eutectic structure did not change much; solely a slight coarsening of the microstructure is observable. In both areas, no elements of the base material were found (see Table 6).

The microstructure of a sample brazed with the same amplitude of the ultrasonic stimulation and an increased activation time of 25 s is shown in Fig. 3B. The increase of the activation time led to a significant change of the appearance of the microstructure. In contrast to the microstructure in Fig. 3A, the sample features one more phase. Besides the dark-grey silver-poor phase and the eutectic phase mixture, another light grey phase is present (4). This phase has a globular shape and comprises of high amounts of Ag as well as Zn and O. The ratio of the eutectic phase mixture has decreased, and its acicular structure is less pronounced.

The use of a high amplitude (38  $\mu\text{m}$ ) and a short activation time of the ultrasound during brazing lead to the formation of an additional phase as well (see Fig. 3C (6)). The silver-poor phases still feature a globular structure, but are significantly smaller in size. A noticeable amount of oxides

**Fig. 2** Microstructure of the braze metal of a sample brazed without the use of ultrasound (cross section parallel to the fracture mirror)

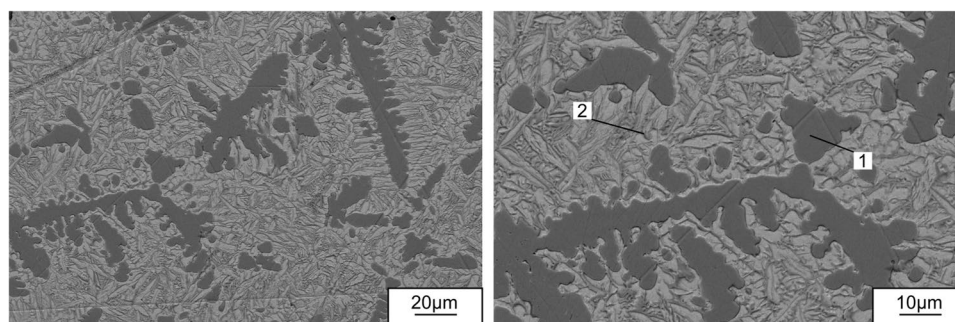


**Table 5** Chemical composition of the braze metal shown in Fig. 2 (values in wt.%)

Point	O	Mn	Fe	Co	Ni	Cu	Zn	Ag	Phase
1	-	19.2	-	-	29.1	21.9	36.2	3.6	Ag-poor
2	6.3	4.7	-	-	3.3	15.9	20.6	49.3	Ag-rich

**Fig. 3** Microstructure of brazing seam (fracture surface) brazed with ultrasound: **A** ultrasound amplitude 19  $\mu\text{m}$ , ultrasound activation time 5 s; **B** ultrasound amplitude 38  $\mu\text{m}$ , ultrasound activation time 5 s; **C** ultrasound amplitude 19  $\mu\text{m}$ , ultrasound activation time 25 s; and **D** ultrasound amplitude 38  $\mu\text{m}$ , ultrasound activation time 25 s

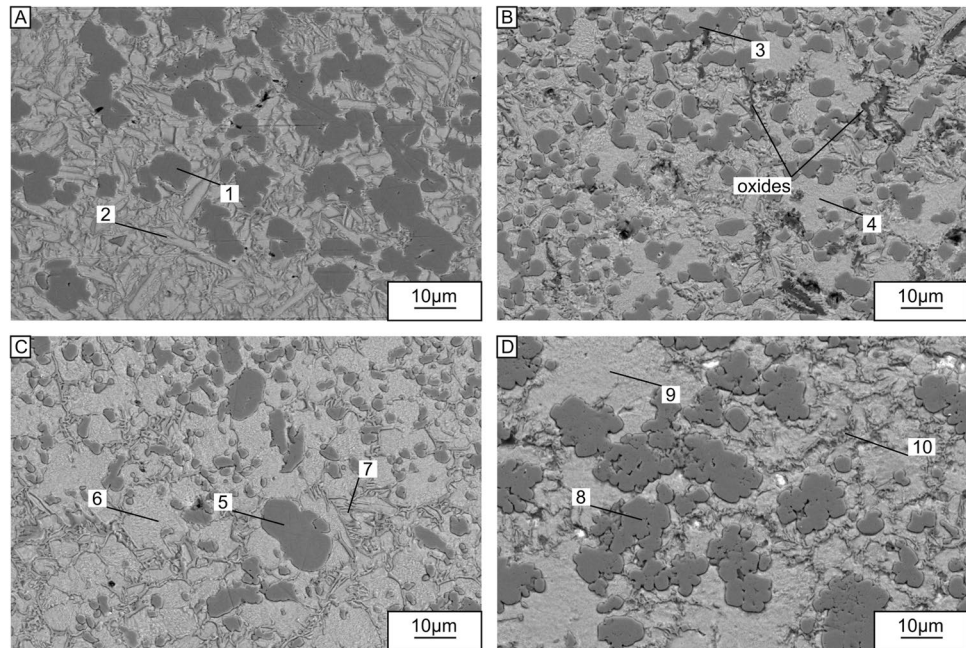


**Table 6** Chemical composition of the braze metal shown in Fig. 3 (values in wt.%)

Point	O	Mn	Fe	Co	Ni	Cu	Zn	Ag	W	Phase
1	-	21.2	-	-	23.8	23.3	28.2	4.5	-	Ag-poor
2	-	4.8	-	-	1.1	8.4	19.3	66.4	-	Eut
3	-	13.8	-	1.3	23.1	28.5	29.9	3.4	-	Ag-poor
4	9.1	2.1	-	-	0.7	8.6	16.8	62.8	-	Ag-rich
5	-	13.2	-	-	21.7	30.8	29.3	5.0	-	Ag-poor
6	9.1	2.3	-	-	0.7	9.0	18.0	61.0	-	Ag-rich
7	9.1	2.7	-	-	1.6	27.3	27.5	32.0	-	Eut
8	-	13.7	1.4	1.9	20.9	27.7	29.8	4.6	-	Ag-poor
9	3.0	2.5	-	-	-	7.0	16.0	67.1	4.5	Ag-rich
10	7.0	3.1	-	0.6	2.5	25.5	26.6	34.7	-	Eut

can be found in the braze metal and appear as black filaments in the micrograph. It can be assumed that the oxides are remnants of broken-up oxide scales from the faying surfaces that were destroyed by the aforementioned cavitation processes. Because of the short activation time, the oxides could not flow out of the brazing gap and remained there during solidification.

The microstructure of the braze metal of a sample brazed with the long activation time of 25 s and the highest amplitude of 38  $\mu\text{m}$  is shown here. The braze metal consists of eutectic phase mixture and two additional phases as well. In contrast to the sample shown in Fig. 3C, no significant existence of remnants of the oxide scales are visible in the cross section of the sample brazed with the same amplitude and a long activation time. Furthermore, it is noticeable that the silver poor phases agglomerated to form bigger areas. The globular silver-rich phases appear to be bigger as well (see Fig. 3D (8)).

The investigation of the composition of the phases shows that the use of a high amplitude (38  $\mu\text{m}$ ) and activation times (25 s) led to a diffusion of the elements Co from the carbide and Fe from the steel (Table 6 (3, 8, 10)). Only Co could be detected in the brazed seam of the samples with a high amplitude and a low activation time. In all other specimen, no elements from the base materials were found.

The cross sections of the samples brazed with ultrasonic stimulation are shown in Fig. 4. The silver-poor phase shows a globular structure in the middle of the brazing seam and forms a continuous band at the interface to the steel. The formation of the layer at the interface can be explained by the high affinity of Ni to Fe in the steel (14). The ultrasound parameters not only have an impact on the phases and their appearance in the braze metal, but on the thickness of the brazing seam and on the content of the base material elements Fe and Co inside the braze metal as well (see Table 7). The samples that were brazed with a high amplitude of

**Fig. 4** Microstructure of brazing seam (cross section) brazed with ultrasound: **A** ultrasound amplitude 19  $\mu\text{m}$ , ultrasound activation time 5 s; **B** ultrasound amplitude 38  $\mu\text{m}$ , ultrasound activation time 5 s; **C** ultrasound amplitude 19  $\mu\text{m}$ , ultrasound activation time 25 s; and **D** ultrasound amplitude 38  $\mu\text{m}$ , ultrasound activation time 25 s

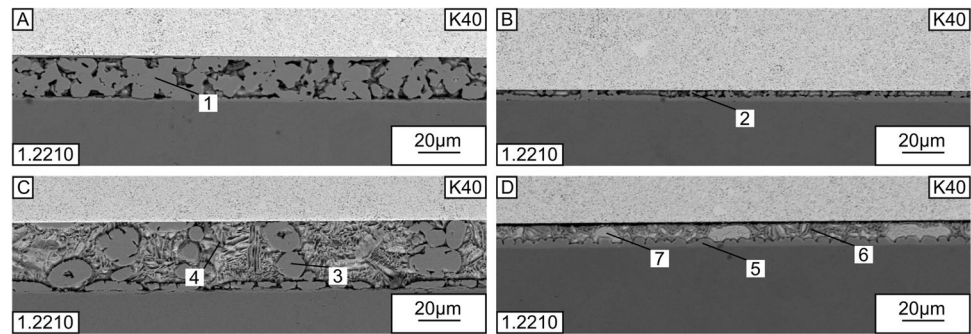


**Table 7** Chemical composition of the braze metal shown in Fig. 2 (values in wt.%)

Point	Mn	Fe	Co	Ni	Cu	Zn	Ag	Phase
1	19.7	1.5	1.0	25.9	23.2	25.4	3.4	Ag-poor
2	12.3	4.1	2.2	19.6	27.6	28.7	2.9	Ag-poor
3	19.6	0.9	-	28.8	21.9	26.2	2.6	Ag-poor
4	5.4	-	-	2.4	26.8	29.0	36.4	Eut
5	15.6	8.6	1.2	23.6	22.7	25.7	2.5	Ag-poor
6	4.4	1.1	-	3.6	26.1	27.7	37.1	Eut
7	2.7	-	-	-	7.6	17.7	72.1	Ag-rich

38  $\mu\text{m}$  (see Fig. 4B and 4D) feature a smaller thickness of the brazing seam than the samples with a lower amplitude. A higher activation time generally led to an increase of the thickness of the brazing seam.

The amounts of the elements Fe and Co differ in the silver-poor phase. Higher amplitudes during brazing led to higher amounts of Fe and Co in the brazing seam (see Table 7 (2, 4)). This can be attributed to the diffusion-promoting effect of the ultrasound and to the shorter diffusion distance because of the thinner brazing seam thickness. The comparably high contents of Fe in the braze metal of the samples brazed with the long activation time emphasize the assumption that ultrasonic stimulation enhances diffusion. A gradient of the Fe and Co could not be detected.

### 3.2 Connectivity

In order to determine the quality of bonds, ultrasonic inspection of the joints has been conducted in immersion technique. Within the test, the reflection of ultrasound that was previously introduced into the sample is measured. The higher the measured signal, the worse the quality of the connection is. Hence, a good bonded area appears to be blue or green. Bad connections appear to be red or orange. The reason for a bad connectivity can be pores and oxides [9]. The specimen that was brazed without the influence of ultrasound has the poorest connection. The lack of bonding in the specimens is 48% of the total brazing area. Samples brazed with a short ultrasonic activation time show a significantly better wetting of about 30%. At an activation time

of 25 s, only very few defects can be detected in the brazing seam. The best bonding is obtained in the samples where the brazing process was supported by ultrasound, which had an amplitude of 19  $\mu\text{m}$  and an activation time of 25 s. The results show that a longer activation time can improve the connectivity inside the brazing seam by destroying oxide layers at the interfaces of the filler metal and the base materials (Fig. 5).

### 3.3 Shear strength

Finally, the obtained shear strength values as arithmetic average of each three samples are shown in Fig. 6 in dependence of the applied ultrasound parameters. In good agreement with the non-destructive ultrasonic immersion testing, the highest shear strength was obtained for a long activation time of 25 s and low amplitude of 19  $\mu\text{m}$ . The maximum average shear strength is 195.0 MPa. The lowest shear strength was obtained for samples without the use of ultrasound. An amplitude of 19  $\mu\text{m}$  leads to the highest strengths regardless of the activation time. The variation of the amplitudes has a minor influence on the joint strength. A correlation of the connectivity and the shear strength is not found. This does not mean that there is no influence of the connectivity on the shear strength. But there are other effects that influence the shear strength, too. For example, the Ag-rich phase that appears in the brazing seam of the samples 25s\_19 $\mu\text{m}$  can lead to a reduction of the shear strength and equalizes the strengthening

**Fig. 5** Missing connectivity of the filler metal to the base material depending on the ultrasound parameter activation time and amplitude (WUS, without ultrasound)

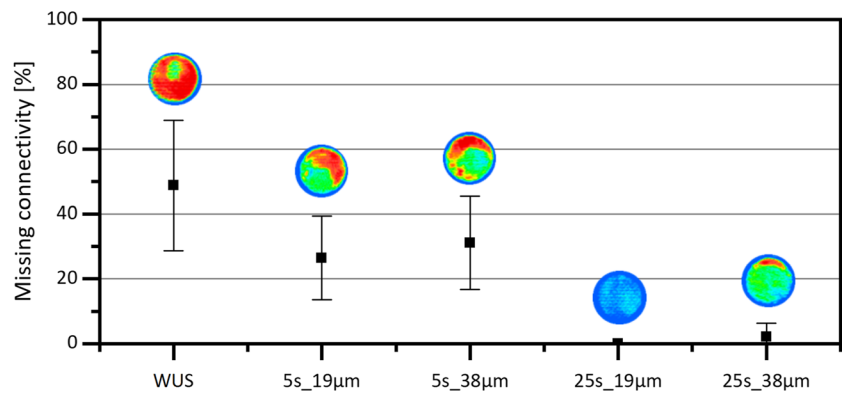


**Fig. 6** Shear strength of the joints depending on the ultrasound parameter activation time and amplitude (WUS, without ultrasound)

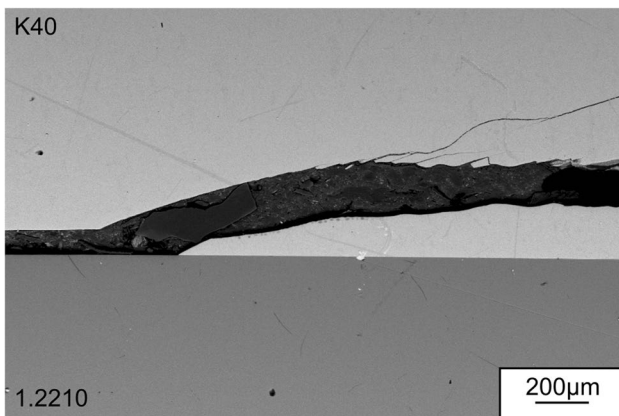
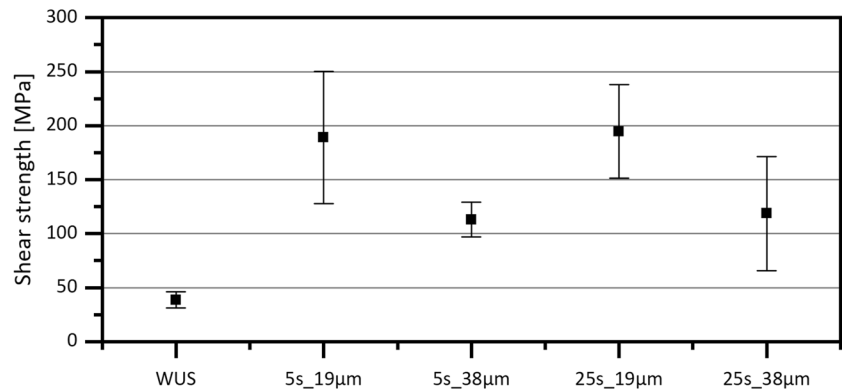


**Fig. 7** Fracture of a 25s\_38µm sample in the cemented carbide

effect of improvement wetting compared to the samples 5s\_19µm. A similar effect was described in [14]. The low shear strength of the 25s\_38µm samples is most probably caused by a failure of the cemented carbide (see Fig. 7). In contrast, the other samples failed in the brazing seam. Furthermore, the presence of oxides and pores in the brazing seam can lead to a lower shear strength, too [9].

## 4 Conclusion and outlook

In this work, ultrasonic-assisted brazing was used to produce flux-free cemented carbide/steel joints in ambient atmosphere. The influence of ultrasound on the microstructure, the bonding, and the joint strength were investigated. The ultrasonic parameters activation time and amplitude of the ultrasonic stimulation were varied, and their influence on the joint microstructure, connectivity and bond strength was analyzed.

1. Ultrasonic stimulation during brazing affects the microstructure of the braze metal. The ultrasound prevents the formation of dendritic structures of the silver-poor phase. In addition, a segregation of phases is visible.
2. The use of ultrasound increases the bonding between the braze metal and the base materials with increasing activation time.
3. The lowest joint strength was obtained for samples brazed without the use of ultrasound. An average strength of only 38.6 MPa was reached. The use of ultrasound during brazing increased the joint strength significantly. The highest strength could be obtained for samples with an amplitude of the ultrasound of 19 µm.

The maximum average shear strength was 195 MPa. An increase of the amplitude of the ultrasound to 38  $\mu\text{m}$  resulted in a decrease of the joint strength.

**Acknowledgements** The authors gratefully acknowledge the financial support of the German Research Foundation (DFG) for the project TI343/158-1, within these findings were obtained.

**Funding** Open Access funding enabled and organized by Projekt DEAL. The study was financially supported by the German Research Foundation (DFG). This work results from the project TI343/158-1.

## Declarations

**Conflict of interest** The authors declare no competing interests.

**Open Access** This article is licensed under a Creative Commons Attribution 4.0 International License, which permits use, sharing, adaptation, distribution and reproduction in any medium or format, as long as you give appropriate credit to the original author(s) and the source, provide a link to the Creative Commons licence, and indicate if changes were made. The images or other third party material in this article are included in the article's Creative Commons licence, unless indicated otherwise in a credit line to the material. If material is not included in the article's Creative Commons licence and your intended use is not permitted by statutory regulation or exceeds the permitted use, you will need to obtain permission directly from the copyright holder. To view a copy of this licence, visit <http://creativecommons.org/licenses/by/4.0/>.

## References

1. Yu X-Y, Zhou D-R, Yao D-J et al (2016) Fiber laser welding of WC-Co to carbon steel using Fe-Ni Invar as interlayer. *Int J Refract Metal Hard Mater* 10:76–86
2. Xu P, Zhou D, Li L (2017) Fiber laser welding of WCCo and carbon steel dissimilar materials. *Weld J* 96:1–10
3. Zhang XZ, Liu GW, Tao JN et al (2017) Vacuum brazing of WC-8Co cemented carbides to carbon steel using pure Cu and Ag-28Cu as filler metal. *J Mater Eng Perform* 2:488–494
4. Zhang X, Liu G, Tao J et al (2018) Brazing of WC–8Co cemented carbide to steel using Cu–Ni–Al alloys as filler metal: microstructures and joint mechanical behavior. *J Mater Sci Technol* 7:1180–1188
5. Akbari Mousavi SAA, Sherafati P, Hoseinion MM (2012) Investigation on wettability and metallurgical and mechanical properties of cemented carbide and steel brazed joint. *Adv Mater Res* 759–764
6. Huang S, Long W, Lu Q et al (2019) Research on the corrosion resistance of Cu-Al joints brazed with flux-cored Zn-2Al filler metal. *Mater Res Express* 5:56560
7. Chen X, Yan J, Gao F et al (2013) Interaction behaviors at the interface between liquid Al-Si and solid Ti-6Al-4V in ultrasonic-assisted brazing in air. *Ultrason Sonochem* 1:144–154
8. Li Y, Zhu Z, He Y, Chen H, Jiang C, Han D, Li J (2016) WC particulate reinforced joint by ultrasonic-associated brazing of WC-Co/35CrMo. *J Mater Process Technol* 238(16):15–21
9. Tillmann W, Ulitzka H, Ulitzka T, Wojarski L, Morozov A (2021) Effect of US-activation time and temperature on cemented carbide-steel joints, *International Brazing and Soldering*
10. Jiang C, Chen H, Wang Q, Li Y (2015) Effect of brazing temperature and holding time on joint properties of induction brazed WC-Co/carbon steel using Ag-based alloy. *J Mater Process Technol* 229(2016):562–569
11. Li Z, Xu Z, Zhao D, Liu X, Yan J (2019) Grain refinement caused by intensified cavitation within narrow channel and its improvement to ultrasonically soldered Al joint property. *Ultrasonic Sonochem* 60:104786
12. Atamanenko TV, Eskin DG, Zhang L (2010) Criteria of grain refinement induced by ultrasonic melt treatment of aluminum alloys containing Zr and Ti. *Metall Mater Trans A* 8(2010):2056–2066
13. Wojarski L., Ulitzka H., Rass I., Tillmann W., et al. (2022) Flux-free joining of dissimilar materials, *LÖT 2022 - 13th Conference on Brazing, High Temperature Brazing and Diffusion Bonding, DVS-Berichte, Band 381, 153–161*
14. Jiang C, Chen H, Wang Q, Li Y (2016) Effect of brazing temperature and holding time on joint properties of induction brazed WC-Co/carbon steel using Ag-based alloy. *J Mater Process Technol* 229:562–569

**Publisher's note** Springer Nature remains neutral with regard to jurisdictional claims in published maps and institutional affiliations.